PROBABILITY DENSITY OF LIGHT FLUX FLUCTUATIONS IN A NARROW DIVERGENT LASER BEAM UNDER SNOWFALL CONDITIONS

N.A. Vostretsov and A.F. Zhukov

Institute of Atmospheric Optics,
Siberian Branch of the Russian Academy of Sciences, Tomsk
Received June 29, 1995

We analyze here measurement results on the probability density distribution of a signal in a narrow divergent laser beam in a snowfall at different diameters of the receiver. The distribution shape depends on the receiver size, optical thickness, and maximum size of the snow particles. The experimental distributions in the majority cases can be described by Γ and normal distributions.

1. INTRODUCTION

When calculating certain basic characteristics of laser systems intended for operation through the atmosphere, it is important to know the distribution of the probability density (DPD) of the electric signal fluctuations at the photoreceiver output. It is a well studied subject in the case of turbulent atmosphere without precipitation (see Refs. 1 and 2 and references therein).

Reported in Refs. 3 and 4 are the experimental results on DPD of a laser signal in snowfalls. The measurements have been carried out on a 964-m-long path in a narrow diverging laser beam with a receiver 0.1 or 0.3 mm in diameter. According to findings in Refs. 3 and 4, most of the DPDs are described by the Γ-function with different values of the parameters. Theoretical study of DPD in snowfalls was not carried out at all. Influence of the pathlength and the receiver diameter on the DPD has not been studied experimentally so far. In this paper we analyze the earlier findings[3,4] and the newly obtained measurement results on the probability density of laser signal fluctuations on the paths of 260, 520, and 780 m lengths in a narrow diverging laser beam in snowfalls with the receiver diameter varying from 0.1 to 25 mm.

2. INSTRUMENTATION

Laser radiation from an LGN-25 laser (LG-38, Ref. 3) was directed toward a photoreceiver (FÉU-38), in front of which the diaphragms of different diameters were placed. The radiation reflected from a flat mirrors placed 130 m apart and propagated at altitude of 1.8 m above the ground. The angle of the laser beam divergence was equal to $5 \cdot 10^{-4}$ rad, and the initial beam radius at half-maximum was 3 mm. The receiver was set on the laser beam axis visually. The receiver's field of view was two orders of magnitude greater than the angle of the laser beam divergence. The optical thickness (τ) was calculated from the data obtained with a visibility range meter (RDV-3). It operated on the 2×100 m path near the laser beam. Maximum size of snow flakes D_m was estimated visually on a 30×30 cm fur surface.

The signal from FÉU output was amplified and then simultaneously directed to the dispersiometer, the correlator, the analyzer of the temporal spectrum, and the pulse-height analyzer AI-1024, with the help of which the probability density of laser signal fluctuations was measured.

The pulse-height analyzer AI-204 is intended for measurements of the output signals of 0.2 to 10 V amplitudes. In this connection, an additional constant signal just higher than 0.2 V was introduced into the input signal in order to provide a possibility of measuring deep fadings of the signal. In our measurements the analysis usually lasted 50 s. Only those DPDs were analyzed, which have been obtained at close values of the atmospheric transmittance on the 2×100 m path. This was checked by the pointer of an RDV-3. Measured were slightly correlated samples of the laser signal. The sample duration was 1 μs, and the sample repetition rate was 1.6 kHz. The pulse analyzer was controlled with a sinusoidal signal, Gauss noise, and random laser signal in the turbulent atmosphere without precipitation, when fluctuations are distributed according to the lognormal law.[1,2,5]

The device generated the expected distributions. The information about the probability of fluctuations was printed out and displayed on an oscilloscope, in the form of a curve — a small-step histogram.

The measurements were conducted near Tomsk in 1993—1994 on the 260 m path during 21 snowfalls, in 1994—1995 on the 520 m path during 26 snowfalls, and in 1995 on the 780 m path during 3 snowfalls.

3. MEASUREMENT RESULTS

Altogether about 290 distributions (including 100 distributions obtained on 964 m path[3]) were measured. By observing histograms on the oscilloscope during the measurements in different snowfalls, it was found that the histogram shapes essentially depend on the receiver

0235-6880/95/12 997-07 $02.00

diameter (D_r), the optical thickness (τ), and the maximum size of snow flakes (D_m). At the same time, we did not find a marked effect of the pathlength on the DPD.

Various combinations of the optical thickness and maximum particle size are possible in snowfalls. They are independent of experimenter's desire, and they cannot be unambiguously predicted. These circumstances make the problem for DPD at various D_r much more complicated for solving with the use of single-channel measurement procedure we have used. In fact the problem expands (by the number of D_r values) as compared to the problem of intensity fluctuations (D_r = 0.1 or 0.3 mm) measurements.[3]

Usually we conduct the measurements of signal statistical characteristics with a certain receiver diameter in different snowfalls, continuously recording the information about τ and occasionally about D_m. However we have always estimated D_m when it changed markedly. Such changes in D_m can be readily found in daytime by simply observing the falling particles against a dark screen. At night first information about the marked change in D_m was obtained by observing particles in the illuminated volume near the window. In addition, the forward scattered radiation of the remote parts of a laser beam could be clearly observed. Changes in the twinkling of this parts were indicative of evolution in the structure of particles. Moreover, an experienced operator can detect marked changes in D_m from the temporal spectrum displayed on a screen of a spectrum analyzer and from the fine structure of a signal displayed on the oscilloscope. However, these ways are not ideal, giving errors in D_m estimates. To reduce the number of errors, we always estimated D_m when measuring DPD. It is difficult to exclude the errors in this part of measurements at all, because D_m can rapidly change even during the DPD measurements.

Measurements with different D_r at close values of both τ and D_m were not necessarily successful, but several favorable situations were observed in our experiments.

To find an analytical expression describing the empirical distributions obtained, we used, as early,[3,4] graphical representation of the probability, according to which experimental data were plotted on a special paper, designed for a chosen distribution. In other words, we used the well-known method of rectified diagrams. The best fit of the experimental data to the straight line serves as the criterion of fulfillment of the distribution.

Five model distributions were studied, namely, lognormal, Rice–Nacagami, exponential (e), normal (n), and gamma (Γ) distributions.

Excluding only 12 experimental distributions, we succeeded in describing the remaining ones with the help of the latter three functions.

The probability density is described by the function

$$P(I) = \frac{1}{\Gamma(\alpha + 1)\beta^{\alpha+1}} I^{\alpha} \exp(-I/\beta), \quad (1)$$

for the gamma-distribution at $I > 0$ (see Ref. 6), where $\alpha > -1$, $\beta > 0$, and $\Gamma(\alpha+1)$ is the Γ-function (equal to $\alpha!$ for integer λ); and

$$P(I) = a \exp(-a I), \quad (2)$$

for the exponential distribution at $I > 0$, where $a > 0$.

Since the shape of Γ-distribution depends on α, it is impossible to construct the probability scale, on which any gamma-distribution could be represented by a straight line. For Eq. (1) the scale grid on the ordinate was constructed following the procedure described in Ref. 6, and for Eq. (2) it was constructed according to the procedure from Ref. 7.

Figure 1*a* demonstrates the change in the shape of the distribution for the 520 m path as a function of a receiver diameter in one of the snowfalls, in which both τ and D_m varied only slightly during the measurements. In this figure, the normalized probability density is shown on the ordinate. It was normalized to its maximum value (P_m). In this snowfall the particle size did not exceed 3 mm.

Figure 1*b* presents the same curves for 780-m-long path, but in this case the optical thickness varied over a wide region from 1.4 to 2.2. In this snowfall we observed some flakes with the maximum size up to 20 mm, as well as far smaller particles with the size as small as 1 mm.

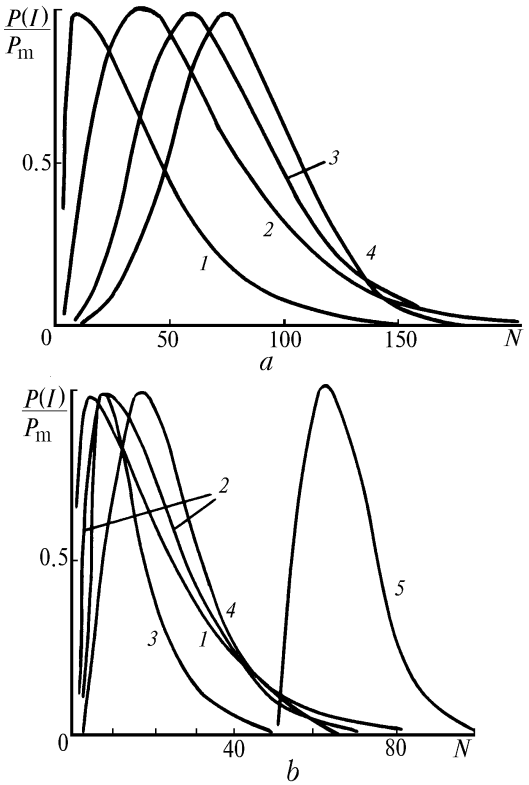

FIG. 1. Distribution of the normalized probability density of light beam fluctuations as functions of D_r.

TABLE I.

Date	σ	τ	D_m	D_r	L	α	Figure	Curve
20.11.94	0.75	1.00	1-3	0.1	520	1	1 *a*	*1*
–	0.55	1.10	–	3.1	–	2	–	*2*
–	0.39	0.90	1	10	–	6	–	*3*
–	0.24	1.00	1-2	25	–	n.l.	–	*4*
10.03.95	0.86	1.70	1-20	0.1	780	1	1 *b*	*1*
–	0.78	1.40	–	0.8	–	1	–	*2*
–	0.72	2.40	–	2	–	1	–	*3*
–	0.35	2.10	–	10	–	8	–	*4*
	0.20	2.20	–	25	–	10	–	*5*
	0.35	1.50	5-10	25	520	9	2 *a*	*1*
	0.42	1.20	–	–	–	7	–	*2*
	0.34	1.00	–	–	–	n.l.	–	*3*
	0.27	0.45	–	–	–	n.l.	–	*4*
	0.19	0.36	–	–	–	no	–	*5*
	0.21	1.20	1-2	25	520	1	2 *b*	*1*
	0.25	0.70	–	–	–	2	–	*2*
	0.16	0.50	–	–	–	4	–	*3*
	0.08	0.20	–	–	–	5	–	*4*
	0.24	0.80	–	–	–	3	–	*5*
21.11.94	1.06	2.00	10	0.1	520	7	3 *a, b*	*1*
27.11.94	0.95	2.04	5	–	520	–	–	*2*
10.03.95	0.86	1.70	1-20	–	780	–	–	*3*
10.03.95	0.61	2.63	1-30	3.1	780	1	4 *a*	*1*
–	0.80	2.08	1-20	1.5	–	–	–	*2*
–	0.79	1.37	–	0.8	–	–	–	*3*
–	0.86	1.70	–	0.1	–	–	–	*4*
20.02.95	0.59	0.52	3-10	0.65	520	3	4 *b*	*1*
–	–	–	2-10	3.1	–	–	–	*2*
04.11.93	0.42	0.64	1-3	3.1	260	7	4 *c*	*1*
29.11.93	0.39	0.20	1-2	3.1	–	–	–	*2*
09.11.93	0.36	0.17	2-3	1.5	–	–	–	*3*
09.11.93	0.26	0.09	1	1.5	–	–	–	*4*
04.11.93	0.37	0.31	2-3	0.8	–	–	–	*5*
09.11.93	0.40	0.32	2-3	0.1	–	–	–	*6*
20.02.95	0.56	0.55	1-20	0.8	520	7	4 *d*	*1*
25.11.94	0.36	0.41	1-3	0.1	–	–	–	*2*
20.02.95	0.51	0.54	2-20	3.1	–	–	–	*3*
04.02.94	0.47	0.77	1-2	3.1	260	7	4 *e*	*1*
03.01.94	0.55	0.67	1-2	0.8	–	–	–	*2*
09.11.93	0.43	0.22	2-5	1.5	–	–	–	*3*
02.11.93	0.30	0.40	1-2	1.5	–	–	–	*4*
04.01.94	0.50	0.40	3-5	0.8	–	–	–	*5*
29.11.93	0.31	0.19	1-2	0.8	–	–	–	*6*
10.03.95	0.27	2.18	1-2	25	780	10	4 *e*	*1*
20.02.95	0.43	0.46	2-10	10	520	–	–	*2*
28.11.94	0.26	0.76	1-2	25	–	–	–	*3*
20.02.95	0.28	0.27	2-3	3.1	–	–	–	*4*
28.11.94	0.26	0.81	1-2	25	–	–	–	*5*
25.11.94	0.01	0.27	1-2	25	520	n.l.	5 *a*	*1*
–	0.04	0.36	–	10	–	–	–	*2*
–	0.01	0.27	–	25	–	–	–	*3*
–	0.04	0.55	–	25	–	–	–	*4*
21.11.94	0.22	1.50	2-3	25	520	n.l.	5 *b*	*1*
01.12.93	0.20	0.10	2	0.8	260	–	–	*2*
21.11.94	0.22	1.59	1-3	25	520	–	–	*3*

TABLE I (continued).

Date	σ	τ	D_m	D_r	L	α	Figure	Curve
01.12.93	0.19	0.10	2-3	0.8	260	—	—	*4*
17.01.94	0.33	0.24	1-3	0.1	—	—	—	*5*
29.11.93	0.40	0.27	3-4	0.8	260	n.l.	5*c*	*1*
02.11.93	0.19	0.29	2	3.1	—	—	—	*2*
—	0.21	0.28	1	2.0	—	—	—	*3*
—	0.16	0.07	1	0.1	—	—	—	*4*
09.11.93	0.43	0.21	2-5	1.5	—	—	—	*5*
	0.09	0.41	1-2	3.1	260	n.l.	5*d*	*1*
	0.20	0.10	—	0.8	—	—	—	*2*
	0.12	0.17	—	10	—	—	—	*3*
	0.21	0.40	—	1.5	—	—	—	*4*
	0.14	0.17	—	10	—	—	—	*5*

*n.l. denotes the normal law.

As is seen from the figures and the table, the level of fluctuations σ decreases with increasing D_r, whereas the parameter of Γ-distribution increases. The latter is typical for Γ-distribution, since the lower levels of fluctuations correspond to Γ-distributions with higher values of the parameter α (Refs. 3 and 4). If $D_r \ll D_m$, the curve is symmetrical and normal law is satisfied quite well.

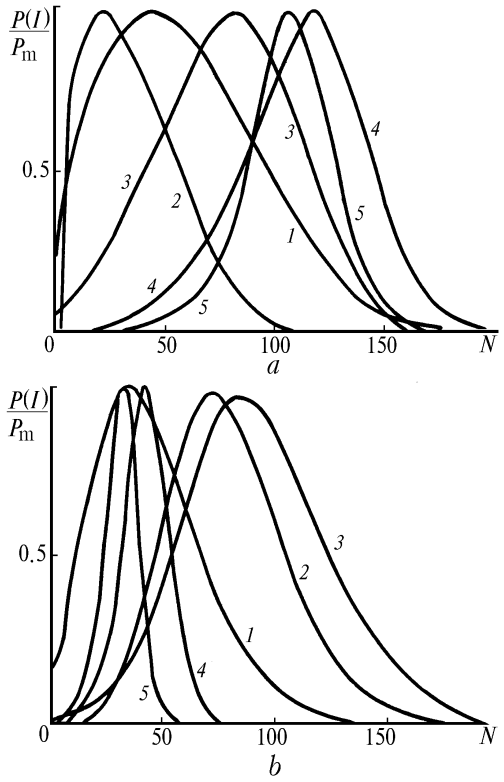

FIG. 2. Distribution of the normalized probability density of light beam fluctuations as functions of D_m and τ at D_r = 25 mm.

Figures 2*a* and *b* demonstrate the change in the shape of distributions for D_r = 25 mm on 520-m-long path with a decrease in the optical thickness in two snowfalls essentially different in D_m, namely, with precipitation of flakes and finely dispersed particles.

It is clearly seen from Figs. 1 and 2 that distributions can have left, right, and nearly symmetric shape.

Figures 3*a* and *b* show the results of DPD measurements at D_r = 0.1 mm for the case of flakes precipitating and the result of check of the exponential distribution. With only flakes (when $D_r \ll D_m$) in a heavy snowfall (τ = 2), this distribution is well satisfied.

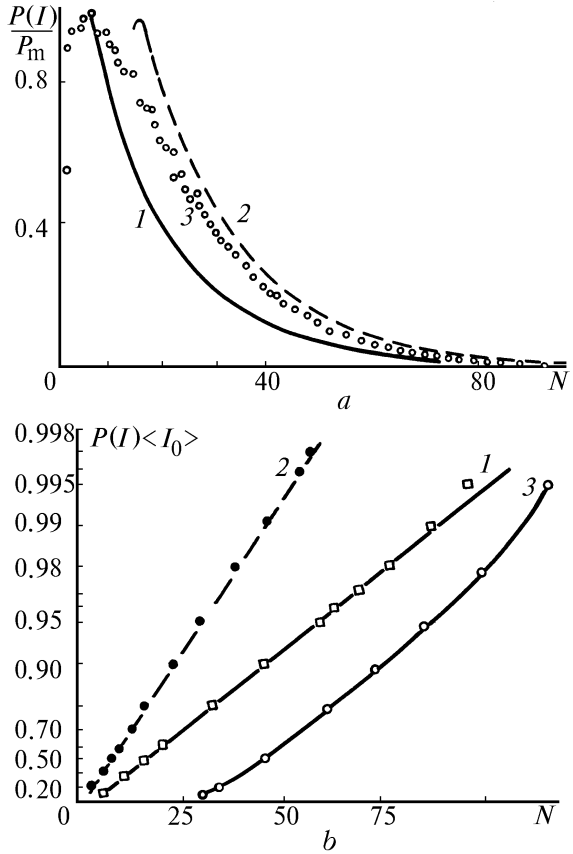

FIG. 3. Examples of description by exponential distribution.

Below we present some examples (Fig. 4) of almost ideal description of empirical distributions by gamma-function with different values of α. Some curves are somewhat shifted to the right, because they can be very close to each other. In Fig. 4 the pathlength is given in meters, and the receiver diameter is given in millimeters. As follows from the figure, the empirical distributions at varying conditions on the path and the receiver diameter can be described by changing α parameter from 1 to 10. Note, just to remind, that the exponential distribution is the gamma distribution at $\alpha = 0$. It should be noted that the distribution with $\alpha = 10$ well describes nearly symmetric distributions.

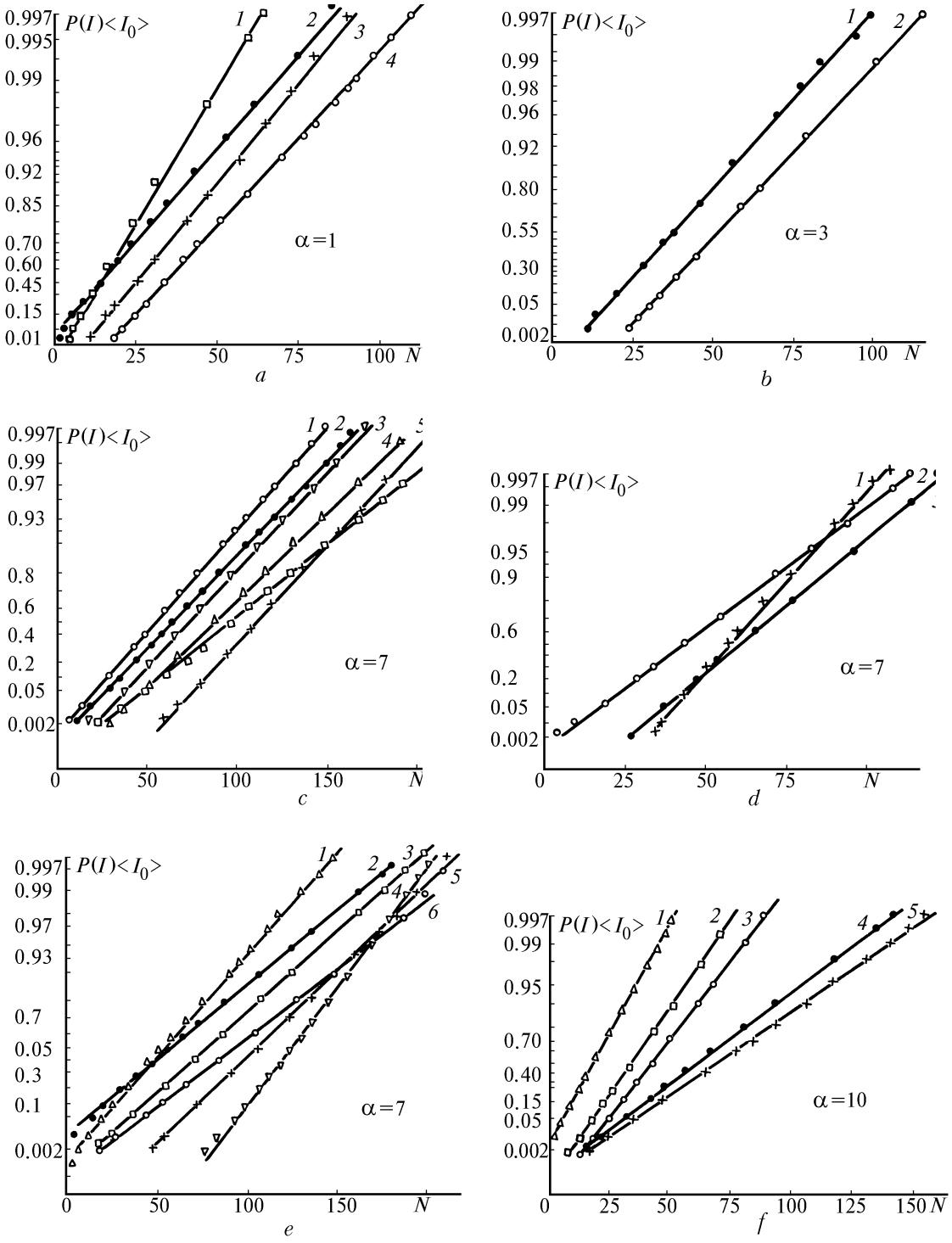

FIG. 4. Verification of the empirical distributions on the closeness to Γ-distribution.

In our measurements, empirical distributions of the probability density were often described by the normal (Gauss) distribution (see Fig. 5). It is valid almost without exceptions when $D_r \gg D_m$. Moreover, in some cases it is also fulfilled, but a little bit poorer, in the region of extreme values of the distribution than at $D_r \gg D_m$ and at small optical thickness ($\tau < 0.4$) and receiver diameter, when D_r is comparable, lower, or somewhat higher than D_m.

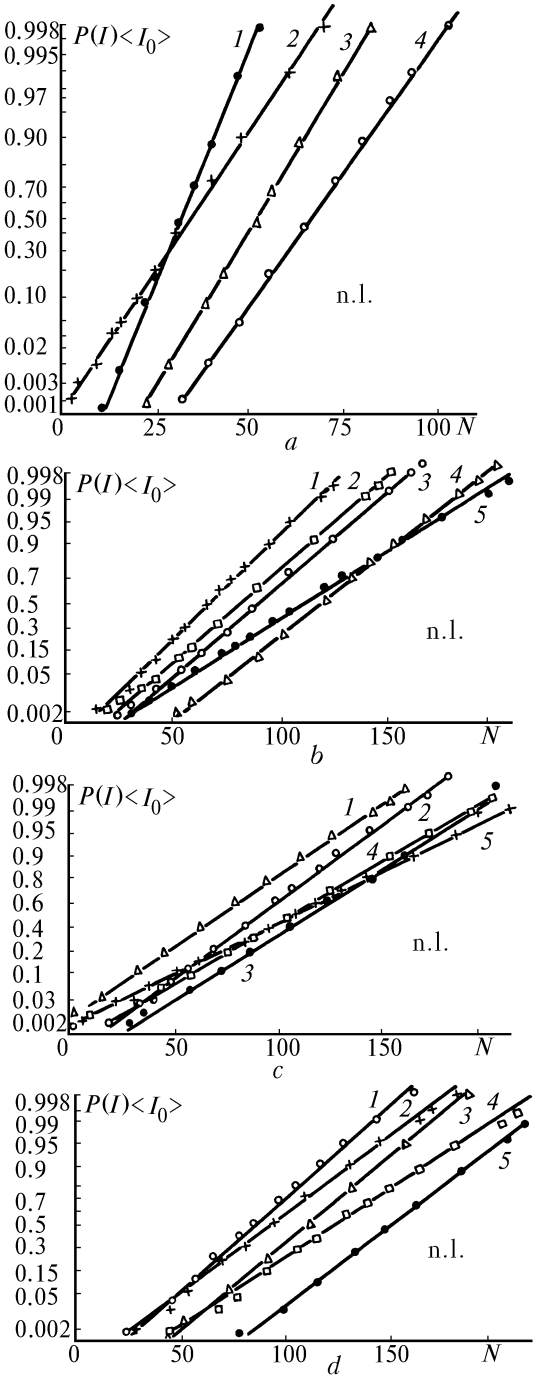

FIG. 5. Comparison of the empirical distributions with the normal law.

The lognormal distribution is in a rather poorer agreement with the experimental data at all values of signal, and the Rice–Nacagami distribution is in a poor agreement with the experimental data only in the region of signal outliners (the right region of extreme values).

4. DISCUSSION

The choice of a distribution, describing the fluctuations of laser signal in the atmosphere, is usually governed by understanding of the fluctuation reasons and is tested by a comparison with experimental data. Such a way is already completed in the case of optical radiation propagation in the atmosphere without precipitation, but up to date there is no logically noncontradictory physical explanation of DPD variations, discovered in experiment over all range of possible variations of the atmospheric parameters.

In precipitation the nature of laser signal fluctuations is different. They are due to simultaneous effect of turbulence and precipitation particles upon the beam. For heavier precipitation, the role of turbulence decreases.[8,9]

An attempt to construct an adequate and rigorous theory of fluctuations under precipitation has failed.[10,11] In order to obtain concrete results in the region of multiple scattering, Borovoi et al.[10,11] had to abandon to take into account all reasons for fluctuations allowing for the most important one — screening of a receiver by particles from the layer adjacent to it.

In a narrow diverging beam, fluctuations are also caused by total or partial interception of a beam by snow particles near a source, because in this case the beam size is comparable with the particle size.[12,13]

Such a simplified approach[12,13] allows a qualitative explanation of the results of scintillation index measurements in snowfalls. Unfortunately, we now cannot define the reasons which govern the nature of Γ-distribution of laser signal fluctuations in precipitation. Wide use of this model is accounted for by the fact that gamma-distribution can take a wide variety of shapes. However, the theoretical justification for applicability of this distribution cannot necessarily be found (see Ref. 14, p. 105). Such is the case with acoustic wave propagation in ocean.[15]

In our opinion, the physical explanation for Γ-distribution fulfillment can be sought within the framework of the following two examples, when it holds.

As follows from Ref. 7, p. 67, use of a Γ-distribution is often justified in problems, where a sum of squares and quadratic forms of normally distributed random values are considered. The light field of laser radiation can be treated as a random

value with regard for interference of scattered waves in the atmosphere.

Following Ref. 16, p. 185, Γ-distribution with parameters α and β results from the combination of α independent random values having exponential distribution with the parameter β. Signals from different sections of a path with different weight in fluctuations according to particle distribution over size can be taken in this example as random values.

Physical nature of Gauss (normal) distribution is well known, and there is no point in discussing it here.

5. CONCLUSION

With a limited number of measurements, which certainly are only a portion of the whole set of possible situations, it is risky to draw the concrete conclusions about DPD. Nevertheless we believe that we have succeeded in revealing, in the first approximation, the characteristic features of DPD for weak and initially strong fluctuations of laser signals in snowfalls. Other peculiar features of DPD are expected to be discovered in the deep scattering mode, when the role of direct unscattered radiation in a signal is small as compared to scattered radiation. At present we have used only one of the known methods for selection of analytical expressions for empirical distributions, i.e., the method of graphical representation of distributions. In the future, other methods will likely be used.

Undoubtedly, in order to gain full understanding of this problem special theoretical investigations are needed in combination with measurements of particle structure, DPD, and turbulence characteristics in precipitation using a specially designed instrumentation. It may become the subject of a separate large research.

ACKNOWLEDGMENT

We would like, in conclusion, to gratefully acknowledge V.N. Krotenko for his help in solving the technical problems and R.Sh. Tsvyk for his help in data processing on a computer.

REFERENCES

1. G.Ya. Patrushev and O.A. Rubtsova, Atmos. Oceanic Opt. **6**, No. 11, 760–769 (1993).
2. S.M. Flatte, C. Bracher, and G.Yu. Wang, J. Opt. Soc. Am. A. **11**, No. 6, 2080–2092 (1994).
3. N.A. Vostretsov, A.F. Zhukov, M.V. Kabanov, et al., Atmos. Oceanic Opt. **6**, No. 1, 22–24 (1993).
4. N.A. Vostretsov and A.F. Zhukov, in: *Abstracts of Reports at the First Inter-Republic Symposium on Atmospheric and Oceanic Optics,* Tomsk (1994), Vol. 1, pp. 160–161.
5. V.I. Tatarskii, *Wave Propagation in a Turbulent Medium* (McGraw-Hill, New York, 1961), reprinted (Dover, New York, 1968).
6. L.M. Levin, *Investigation into Physics of Coarse-Disperse Aerosols* (Academy of Sciences of the USSR, Moscow, 1961), 267 pp.
7. Ya.B. Shor and F.N. Kuz'min, *Tables for Reliability Analysis and Control* (Sov. Radio, Moscow, 1968), 283 pp.
8. N.A. Vostretsov, A.F. Zhukov, M.V. Kabanov, and R.Sh. Tsvyk, *"Statistical characteristics of laser beam intensity fluctuations in snowfalls,"* Preprint No. 13, Institute of Atmospheric Optics of the Siberian Branch of the Academy of Sciences of the USSR, Tomsk (1982), 50 pp.
9. A.F. Zhukov and R.Sh. Tsvyk, Izv. Akad. Nauk SSSR, Fiz. Atmos. Okeana **16**, No. 2, 164–171 (1980).
10. A.G. Borovoi, Izv. Vyssh. Uchebn. Zaved., Ser. Radiofiz. **25**, No. 4, 391–400 (1982).
11. A.G. Borovoi, G.A. Patrushev, and A.I. Petrov, Appl. Opt. 27, No. 17, 3704–3714 (1987).
12. A.G. Borovoi, A.F. Zhukov, and N.A. Vostretsov, J. Opt. Soc. Am. A **12**, No. 5 (1995).
13. A.G. Borovoi, G.A. Patrushev, and A.F. Zhukov, Proc SPIE **1968**, 282–292 (1993).
14. G. Khan and S. Shapiro, *Statistical Models in Engineering Problems* [Russian translation] (Mir, Moscow, 1966), 395 pp.
15. T.E. Ewart, J. Acoust. Soc. Am. **4**, No. 4, 1490–1498 (1989).
16. S. Wilks, *Mathematical Statistics* (Nauka, Moscow, 1967), 632 pp.